Journal of Mechatronics, Electrical Power, and Vehicular Technology 16 (2025) 244-255

Journal of Mechatronics, Electrical Power, and Vehicular Technology

e-ISSN: 2088-6985
p-ISSN: 2087-3379

mev.brin.go.id

Performance study of corncob-fueled updraft gasification with integrated solar power plant as a supporting energy source for the reactor

Rifaldo Pido [a, *], Steven Humena [a, b], Fadhil Abdullah [c]

[a] *Department of Mechanical Engineering, Gorontalo University*
Jl. Ahmad A. Wahab No. 247, Kayubulan, Gorontalo, 96214, Indonesia

[b] *Department of Electrical Engineering, Faculty of Engineering Gorontalo Ichsan University*
Jl. Achmad Nadjamudin, Gorontalo, 96138, Indonesia

[c] *Agricultural Product Technology Study Program, Gorontalo University*
Jl. Ahmad A. Wahab No. 247, Kayubulan, Gorontalo, 96214, Indonesia

Abstract

The increasing demand for energy and the depletion of fossil fuel reserves have accelerated the development of renewable energy sources, with biomass emerging as one of the most promising candidates. Corncobs, an abundant agricultural residue with considerable energy content, represent a viable feedstock for gasification processes. This study evaluates the performance of a corncob-fueled updraft gasifier integrated with a photovoltaic (PV) solar power system as an auxiliary energy source for reactor operation. Experimental tests were conducted to assess flame characteristics, syngas composition, thermal efficiency, and overall energy potential. The influence of air flow rate (AFR) on temperature profiles across the drying, pyrolysis, oxidation, and reduction zones was systematically analyzed. The findings show that low AFR enhances heat accumulation but restricts oxygen supply, whereas excessively high AFR produces cooling effects that reduce thermal efficiency. Optimal operating conditions were achieved at intermediate AFR values (11.5–13.4 m/s), yielding stable heat distribution and high-quality syngas dominated by CO, H_2, and CH_4. Under these conditions, the system demonstrated promising thermal efficiency for small-scale applications. The 600 Wp PV system effectively supplied power to operate the blower, pump, and instrumentation, supporting operational autonomy and reducing reliance on external electricity sources. Overall, the integration of corncob gasification and solar energy offers a sustainable, environmentally friendly, and technically feasible hybrid energy solution, while promoting the utilization of agricultural waste and reducing dependence on fossil fuels in rural areas.

Keywords: biomass gasification; renewable energy; solar hybrid system; updraft gasifier.

I. Introduction

The utilization of biomass as an alternative energy source is increasingly developing in line with the growing energy demand and the limited fossil fuel reserves [1]. Biomass gasification technology, particularly in updraft gasifiers, offers an attractive solution to convert organic materials such as corncobs into syngas that can be used as fuel [2]. Corncobs are one of the agricultural wastes with high potential to be utilized as fuel in the gasification process due to their abundant availability and relatively high energy content.

* Corresponding Author. rifaldopido@unigo.co.id (R. Pido)

https://doi.org/10.55981/j.mev.2025.1312

Received 6 November 2025; 1st revision 1 December 2025; 2nd revision 3 December 2025; accepted 4 December 2025;
available online 26 December 2025

How to Cite: R. Pido *et al.*, "Performance study of corncob-fueled updraft gasification with integrated solar power plant as a supporting energy source for the reactor," *Journal of Mechatronics, Electrical Power, and Vehicular Technology*, vol. 16, no. 2, pp. 244-255, Dec. 2025.

The development and optimization of updraft gasifier performance using biomass are crucial to improve energy conversion efficiency and reduce greenhouse gas emissions [3]. This study aims to analyze the performance of an updraft gasifier using corncobs as fuel through the evaluation of key operational parameters and the characteristics of the syngas produced. The study will also assess the potential applications of the produced syngas for various purposes, including power generation and fuel synthesis, as well as evaluate the economic and environmental feasibility of the corncob gasification process [4]. This research further explores the technical challenges in optimizing the updraft reactor design, particularly those related to gas flow distribution and uniform reaction zones, as well as strategies to mitigate tar formation, which is a major obstacle in syngas utilization [5].

The updraft gasifier is a reactor that allows the gasifying agent to flow counter currently to the solid biomass, sequentially creating drying, pyrolysis, combustion, and reduction zones within a single column, producing syngas rich in hydrogen and carbon monoxide [6]. This design enables the utilization of residual heat from the combustion zone to preheat the incoming biomass, thereby enhancing overall thermal efficiency [7]. In addition, the use of biomass as an alternative fuel can contribute to reducing greenhouse gas emissions due to its carbon-neutral characteristics. This aligns with global efforts to achieve net-zero emissions by 2050 through the increased utilization of renewable energy sources [8]. This study will also include an in-depth thermodynamic analysis of energy conversion efficiency, the variation of product gas composition under different operational conditions, as well as the methane and hydrogen content that are crucial for further applications [9]. Furthermore, the study will examine the sustainability aspects of biomass utilization, including a life cycle assessment to comprehensively measure the environmental impacts of the gasification process [10][11]. It will also cover flame characteristics, product gas composition, thermal efficiency, and the power potential generated from corncob biomass as a renewable energy source. Previous research is shown in Table 1.

The novelty of this research lies in the experimental evaluation of an updraft gasification system fueled by corncob biomass integrated with a PV-based solar energy system, as well as the simultaneous analysis of AFR variations, the temperature profile across each zone, syngas performance, and the adequacy of PV power to support reactor operation. The research gap addressed in this study is the absence of experimental investigations that directly examine the relationship between AFR temperature and syngas in small-scale PV-powered updraft gasification systems.

The objective of this study is to analyze the gasification performance of corncob feedstock in an updraft reactor by observing the temperature distribution, flame stability, and thermal efficiency at various air flow rates (AFR). Additionally, the study aims to evaluate the capability of a 600 WP PV system to supply power for the blower, pump, and instrumentation during the gasification process. This research also seeks to assess the potential integration of PV gasifier technology as a renewable hybrid energy system for household-scale and small industrial applications.

Table 1.
Comparison table with previous studies.

Reference	Reactor & feedstock type	Research result
Martínez *et al.* [12]	Pilot-scale fixed bed gasifier (downdraft); corncob feedstock	By increasing the fine particle content in the feedstock by 15 % and operating the electrical load near its nominal capacity, the reactor temperature rises and the specific fuel consumption decreases (SFC reaches 2.06 kg/kWh at 67 % less point "capacity")
Martillo *et al.* [13]	Experimental downdraft gasifier; agricultural residues incl. corncob	Corncob gasification offers significant renewable energy potential, and its implementation reduces the carbon footprint compared to direct combustion.
Xu *et al.* [14]	Review: various configurations (concentrating solar, hybrid reactors)	Higher temperatures and gasifying agents based on steam or oxygen-enriched air increase syngas yield and the H_2/CO ratio, while pretreatment methods such as torrefaction and the use of multistage air bed gasifiers are recommended to enhance the quality and overall performance of the gasification process.
Xin *et al.* [15]	The concept of integrating solar-thermal + PV with a gasifier (hybrid system)	The system's thermal efficiency increases significantly, fuel production costs can be reduced, and CO_2 emissions decrease substantially compared to conventional scenarios, demonstrating an economical and environmentally friendly solution for large-scale renewable fuel production.
Jadidi *et al.* [16]	Integrated solar-assisted gasification cycle (ISGC) (industrial scale) concept: solar heat to support gasification	The integration of solar-derived heat can reduce fossil fuel consumption and overall emissions, making the ISGC system more sustainable and both technically and economically feasible.

II. Materials and Methods

This research outlines a comprehensive methodology, including the preparation of corncob fuel, the assembly and calibration of the updraft gasification system, as well as the standard operating procedures for performance testing. The method will also address the analysis of experimental data, including syngas composition, conversion efficiency, and gas production rate, in order to thoroughly evaluate the overall system performance. Another aspect to be explored is the potential implementation of the gasification system at the household scale, particularly in rural contexts where agricultural waste is abundant, to meet domestic energy needs and reduce dependence on fossil fuels [17]. This innovation is also expected to provide a solution to environmental problems by utilizing organic waste that has not been optimally managed, while at the same time offering an alternative energy source that is accessible and sustainable [18].

Figure 1 illustrates an energy conversion system based on solar photovoltaic (PV) technology, which is utilized to operate the components required to produce the combustion process (stove/gasifier). This research system begins with the design stage, namely the development of a solar PV-based energy conversion system integrated with combustion supporting components such as a pump, blower, and glow plug, followed by the installation and integration of solar panels, batteries, inverters, and other electrical components to ensure proper functionality according to the design. A functional test is then carried out to verify that each component, including the inverter, pump, blower, and glow plug, operates correctly, after which the combustion test in the reactor or gasifier is conducted to produce a flame. The flame is observed in terms of its color, stability, and temperature. Subsequently, data collection is performed, including voltage and current from the solar panels and batteries, power consumption of each component, flame temperature, and the energy conversion efficiency from PV-generated electricity to thermal energy. Finally, the analysis stage involves comparing the test results with theoretical expectations, evaluating flame stability and system power consumption, and determining the potential application of this system for household energy needs as well as small-scale industrial use. The experimental setup is shown in Figure 2.

A. Fuel consumption rate (FCR)

Fuel consumption rate (FCR) refers to the rate of biomass consumption per unit of time, which directly affects the operational duration of the gasification system and the volume of syngas produced, as defined in equation (1):

$$FCR = \frac{M_T}{\sigma_T} \quad (1)$$

where M_T represents the average biomass consumption per unit of time, reflecting the main tendency or typical consumption during the gasification process, while σ_T denotes the standard deviation that indicates the level of variation or fluctuation in fuel consumption over time. FCR serves as an important parameter in determining the operating duration, process stability, and the volume of syngas produced. This ratio provides an indication of the consistency of the process: the

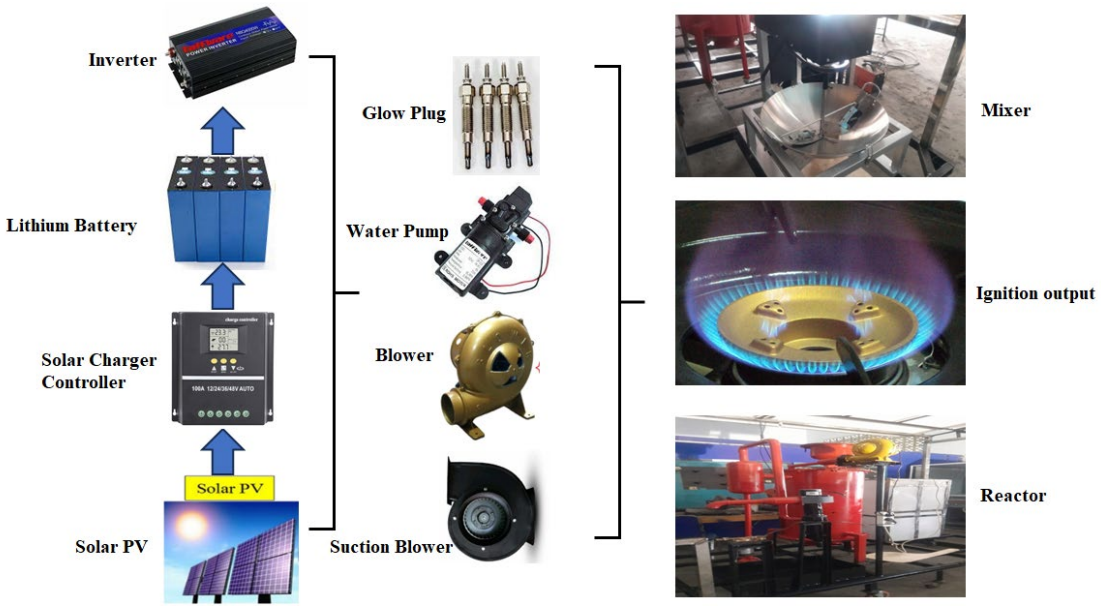

Figure 1. Block diagram of the hybrid energy system of photovoltaic and biomass gasifier.

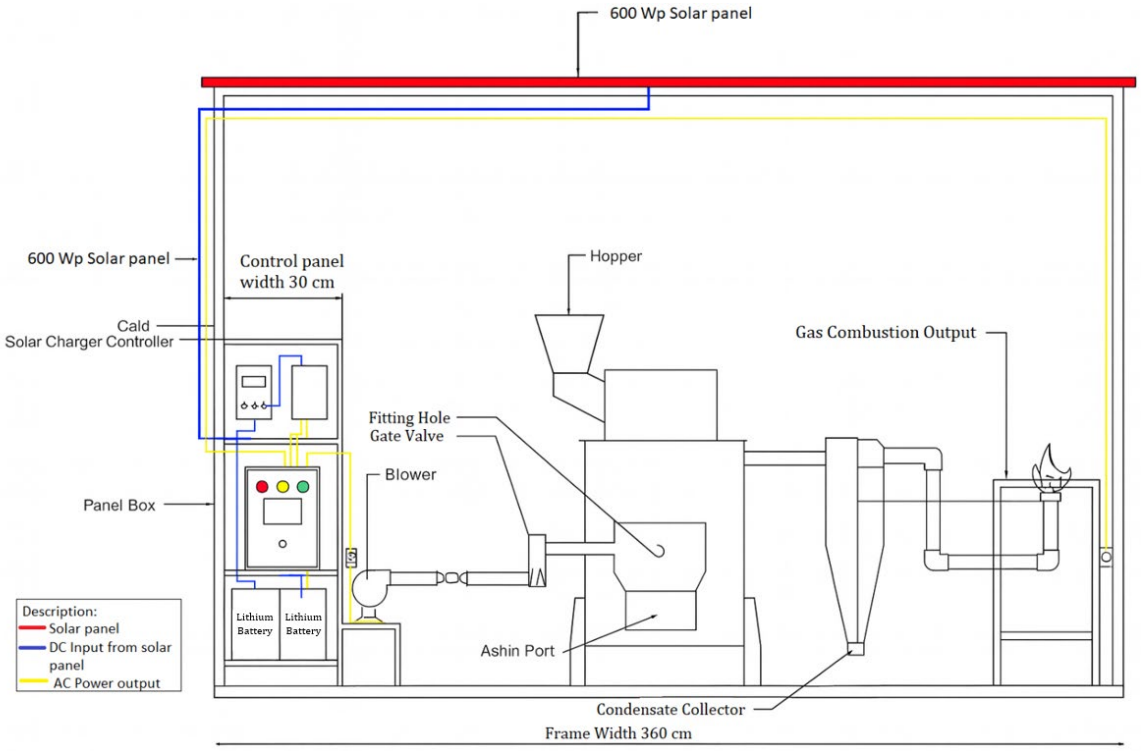

Figure 2. Schematic diagram of the testing apparatus.

higher the FCR value, the more stable and controlled the biomass consumption is, as its variability is relatively small compared to the mean value. Therefore, FCR becomes an essential indicator for evaluating the efficiency and stability of the overall gasification system performance.

B. Sensible heat (SH)

Sensible heat is the thermal energy contained in the producer gas, which can be measured based on the temperature change of the product gas at constant pressure [19]. The calculation of sensible heat is essential for evaluating the thermal efficiency of the gasification process and for designing further heat utilization systems, using equation (2).

$$SH = M_a \times C_p \times (T_{ak} \times T_{aw}) \quad (2)$$

Equation (2) is used to calculate the amount of sensible heat contained in the producer gas, where M_a represents the mass flow rate of the gas or the amount of gas mass leaving the reactor per unit of time, which directly influences the total thermal energy carried by the gas stream. The parameter C_p is the specific heat at constant pressure, which indicates the amount of energy required to raise the temperature of one unit of gas mass by one degree under constant pressure, making it a key factor in determining how much thermal energy the gas can absorb or release. Meanwhile, T_{ak} refers to the actual outlet temperature of the gas, and T_{aw} represents the reference temperature or ambient air temperature. The temperature difference $(T_{ak} - T_{aw})$ illustrates the increase in the gas temperature relative to its initial condition, serving as the basis for calculating the thermal energy contained within the gas. Thus, this equation shows that sensible heat is directly proportional to the gas mass, its heat capacity, and its temperature change, thereby providing a quantitative assessment of the thermal energy that can be utilized or lost in the gasification process.

C. Latent heat (LH)

Latent heat is the energy required to change the phase of a substance without a change in temperature, which in the context of biomass gasification generally refers to the energy stored in the water vapor formed during the process [20]. Quantifying this latent heat is crucial for accurately calculating the thermal efficiency of the system and for designing optimal heat exchangers to maximize overall energy utilization [21], using equation (3).

$$LH = M_a \times H_{fg} \quad (3)$$

Equation (3) is used to calculate the amount of latent heat involved in phase change processes, particularly the evaporation of moisture or water vapor carried within the producer gas stream. In this equation, M_a represents the mass flow rate of the gas or the mass of water vapor undergoing phase change per unit of time, which determines the total amount of latent energy required or released during the process. The parameter H_{fg} refers to the latent heat of vaporization,

which is the amount of energy needed to convert one unit of water mass from liquid to vapor at constant pressure without a change in temperature. By multiplying the mass flow rate of the vapor by its latent heat of vaporization, this equation provides a quantitative estimate of the latent energy involved in the gasification system. This calculation is important because latent heat directly affects the overall energy demand of the process, the thermal efficiency of the gasifier, and the design of heat recovery or downstream energy utilization components.

D. Thermal efficiency (TE)

Thermal efficiency (*TE*) is the ratio between the thermal energy produced in the syngas and the total thermal energy contained in the input biomass, indicating the effectiveness of converting biomass energy into a usable gas [22].

$$TE = \frac{SH + LH}{LHV_t \times M_t} \quad (4)$$

Equation (4) is used to calculate the thermal efficiency (*TE*) of the gasification process by comparing the total usable heat energy with the potential energy contained in the fuel. In this equation, *SH* represents the sensible heat, which describes the thermal energy carried by the producer gas due to an increase in temperature, while *LH* refers to the latent heat associated with the energy required or released during phase change processes, particularly the evaporation of moisture in the fuel. The term LHV_t denotes the total lower heating value of the biomass, which is the amount of energy that can be released from the dry fuel without accounting for the latent heat of vaporization. Meanwhile, M_t represents the total mass of biomass used in the gasification process. By comparing the total utilized heat energy (*SH* + *LH*) with the potential energy of the biomass ($LHV_t \times M_t$), this equation provides a quantitative assessment of how efficiently the gasification system converts the chemical energy of the fuel into usable thermal energy. A higher thermal efficiency indicates that the system is able to utilize a greater portion of the biomass energy effectively.

E. Gasification efficiency

Gasification efficiency is the ratio between the chemical energy contained in the produced syngas and the total chemical energy in the input biomass, thereby representing the efficiency of the biomass conversion process into combustible gas products [23][24], as well as measuring how effectively the gasifier converts solid energy into usable gas.

$$\eta_{gas} = \frac{E_{syngas} \times Duration\ of\ gas\ production}{(E_{air} + E_{corncobs} \times Operation\ time)} \times 100\ \% \quad (5)$$

Equation (5) is used to calculate the gasification efficiency by comparing the total energy produced in the form of syngas with the total energy input supplied to the system. In this equation, E_{syngas} represents the energy contained in the syngas generated during the gasification process, while the Duration of gas production indicates the time span during which syngas is produced. Meanwhile, E_{air}refers to the energy carried by the incoming air, and E_{corncobs} represents the potential energy contained in the biomass fuel, specifically corn cobs. These input energy values are multiplied by the Operation time, which is the total duration of the gasifier's operation. By comparing the output energy with the input energy and multiplying by 100 %, the equation provides the gasification efficiency in percentage form, reflecting how effectively the system converts the energy from biomass and air into usable syngas.

F. Photovoltaic mathematical model

The mathematical model of photovoltaics provides a comprehensive framework for analyzing and optimizing the performance of PV systems by considering various parameters such as solar irradiation, temperature, and device characteristics. This model typically incorporates equations that describe the characteristics of solar panels to predict the energy output and efficiency of the PV system under different operating conditions.

The output power of the PV panel is calculated using equation (6).

$$P_{PV} = f_{PV} \times \frac{I_T}{1000} \times \{1 + \alpha(T_c - T_s)\} \quad (6)$$

Equation (6) is used to calculate the output power of a photovoltaic panel based on the solar radiation intensity and the temperature effect on the solar cells [25]. In this equation, f_{PV} represents the nominal capacity of the PV panel under standard conditions. The value I_T is the total solar irradiance received by the module surface in W/m², which is divided by 1000 to match standard test conditions. The temperature correction factor is expressed through α, the temperature power coefficient, which indicates how temperature changes influence the panel's performance. The parameter T_c is the actual operating temperature of the solar cells, while T_s is the reference standard temperature, usually 25 °C. The temperature difference ($T_c - T_s$) shows how much the operational condition deviates from the ideal state, which affects whether the output power increases or decreases. Therefore, this

equation illustrates how the combination of solar irradiance and thermal conditions determines the actual electrical power produced by the photovoltaic panel.

G. Mathematical gasification model (energy and exergy balance).

The energy efficiency of the gasification process is determined by comparing the energy contained in the produced syngas with the total available energy in the biomass feed and the gasifying agent. Mathematically, energy efficiency is expressed through equation (7).

$$\eta_{energy} = \frac{m_{gas}\, LHV_{gas}}{m_{biomass}\, LHV_{biomass} + H_{agent}} \quad (7)$$

In this equation, m_{gas} represents the mass flow rate of the produced syngas, while LHV_{gas} is its lower heating value. The terms $m_{biomass}$ and $LHV_{biomass}$ denote the mass flow rate and lower heating value of the biomass feedstock, respectively. The term H_{agent} accounts for the energy contribution from the gasifying agent such as air, steam, or oxygen if its energy input needs to be considered.

Meanwhile, the exergy efficiency is calculated based on the ratio between the chemical exergy of the generated syngas and the total exergy supplied by both the biomass and the gasifying agent. Mathematically, exergy efficiency is expressed through equation (8).

$$\eta_{exergy} = \frac{Ex_{gas}^{ch}}{Ex_{biomass} + Ex_{agent}} \quad (8)$$

In this expression, Ex_{gas}^{ch} refers to the chemical exergy of the produced syngas. The term $Ex_{biomass}$ represents the total exergy of the biomass feed, while Ex_{agent} denotes the exergy carried by the gasifying agent. Therefore, the exergy efficiency provides a comprehensive assessment of process irreversibilities and the system's capability to utilize the maximum energy potential of the biomass.

H. Research procedures

1) A brief summary of the purpose of the procedure

Determining the effect of variations in air flow rate (AFR) on: (1) the temperature profile in the drying, pyrolysis, oxidation, reduction zone, (2) the composition and quantity of syngas, (3) thermal and gasification efficiency, and (4) the ability of the PV system to supply operational loads (blowers, pumps, instrumentation).

2) Fuel preparation (corncob)

The corncob used in the test was collected and then cut into 3 – 6 cm particle sizes according to research requirements. The fuel was then naturally dried to a constant weight with a final moisture content of 10–12 % (w.b.) before being stored in a sealed container until the test date. The selection of a particle size of 3 – 6 cm was based on technical considerations to reduce the risk of bridging in the updraft reactor and ensure compliance with laboratory scale, while the moisture content of 10–12 % was chosen to minimize the latent energy requirement for vaporization and represent optimal dry fuel conditions for gasification performance testing. Parameters recorded at this stage included initial mass (g), moisture content (%), particle size (mm), and bulk density (kg/m³).

3) Reactor & instrumentation specifications

The updraft reactor used has an inner diameter of 60 cm and an effective height of 100 cm, made of carbon steel with several supporting components using SS 304 in areas requiring higher temperature resistance. The installed instrument system includes K-type thermocouples with an accuracy of ± 2.2 °C placed in the four main zones of the reactor, namely the drying, pyrolysis, oxidation, and reduction zones, each installed in a fixed position according to the reactor design. The air flow rate is measured using an anemometer mass flowmeter with an accuracy of ±0.1 m/s, while the output gas flow rate is recorded using a calibrated flowmeter. Parameters related to the energy system are recorded using a pyranometer for solar irradiance, a voltmeter and a clamp meter for measuring the voltage and current of the solar panels, as well as a data logger with a recording interval of 1 second to 1 minute. In addition, the determination of the fuel consumption rate (FCR) is carried out using a digital scale with an accuracy of ±0.1 g.

4) Calibration & pre-test check

The instrument calibration procedure was carried out prior to testing to ensure data accuracy. Thermocouples were calibrated using a standard bath at two reference points, an ice bath at 0 °C and boiling water at 100 °C, allowing any deviations to be corrected consistently. The anemometer was calibrated using a wind tunnel or a verified flow standard by comparing instrument readings against reference values at several airflow velocities. The gas flowmeter was calibrated using a volumetric method with a bellows calibrator or flow standard to ensure accurate measurement of the reactor's gas output flow rate. For gas composition analysis, the gas chromatograph (GC) was calibrated using certified standard gas mixtures, such as 1% H_2, 1 % CO, and 1 % CH_4 with N_2 or He as the carrier gas, using at least three calibration points to verify detector linearity before analyzing the samples.

5) Experimental procedure (step by step)

The experiments were conducted at five AFR settings: 7.8, 9.6, 11.5, 13.4, and 15.4 m/s with each condition tested in a minimum of three independent replicates. For every trial, the initial mass of corncob fuel was measured at approximately 2.000 kg (accuracy ±0.005 kg), after which the reactor was filled uniformly while recording the corresponding volume and bulk density. The initiation stage began by activating the PV system to ensure a stable power supply, followed by setting the blower to the desired AFR (or to zero for manual pre-heating if required), and igniting the glow plug or burner to start the gasification reaction while recording the initiation time (T_0). The reactor was allowed to operate until all temperature sensors exhibited fluctuations of less than ±3 % for at least five minutes, which was considered the steady-state condition, and the time to reach this condition was documented. During the steady-state period, data were recorded for 20 – 30 minutes per replicate, consistent with the 0 – 22 minutes water-boiling curve, including zone temperatures at intervals of 1 second to 1 minute, AFR, solar irradiance, PV voltage and current, producer-gas flow rate, and fuel mass measurements if required for fuel consumption rate (FCR) analysis. Syngas samples for GC analysis were collected every 5 minutes, yielding 4 – 6 samples per run, and tar was captured using a condenser or impinger when necessary. After the sampling period ended, the ignition source was turned off, the blower was stopped, the reactor was allowed to cool, and the remaining fuel mass was measured for FCR calculation.

III. Results and Discussions

This study investigated the effect of air flow rate (AFR) on the characteristics of syngas produced from corncob feedstock using an updraft gasifier. AFR variation was implemented by adjusting the blower air valve (blower shown in Figure 3), allowing precise control of oxygen availability within the reactor. The experimental procedure involved systematic observation and data retrieval on several key parameters, including the reactor temperature profile, syngas composition, flame stability, and overall thermal efficiency. Analytical methods were used to process the collected data, allowing a detailed evaluation of the relationship between AFR and gasification performance. This approach provides a comprehensive assessment of how different AFR settings affect the quality and quantity of syngas produced, offering valuable insights for optimizing biomass gasification processes for renewable energy applications.

A. AFR and temperature profile

The temperature profiles in each gasification zone under different air flow rates (AFR) reveal a strong correlation between oxygen supply and heat distribution within the reactor, as shown in Table 2 and Figure 4. At the lowest airflow rate of 7.8 m/s, the peak temperature in the oxidation zone reached its highest value (±820 °C), while the pyrolysis (±500 °C) and reduction zones (±660 °C) also exhibited relatively high temperatures. This condition occurred because the limited air supply reduced convective cooling, allowing more heat from oxidation reactions to accumulate. When the airflow rate increased to 9.6 m/s, the temperatures in all zones dropped significantly, with the oxidation peak decreasing to around 540 °C and the

Table 2.
Temperature in each zone (drying, pyrolysis, oxidation, reduction).

No	Air velocity (m/s)	Zone 1	Zone 2	Zone 3
		Pyrolysis (°C)	Oxidation (°C)	Reduction (°C)
1	7.8	380–560	820	720→600
2	9.6	320–510	540	380→300
3	11.5	330–600	630	600→420
4	13.4	340–650	660	650→410
5	15.4	340–680	700–720	670→360

Figure 3. Blower and anemometer measuring instrument.

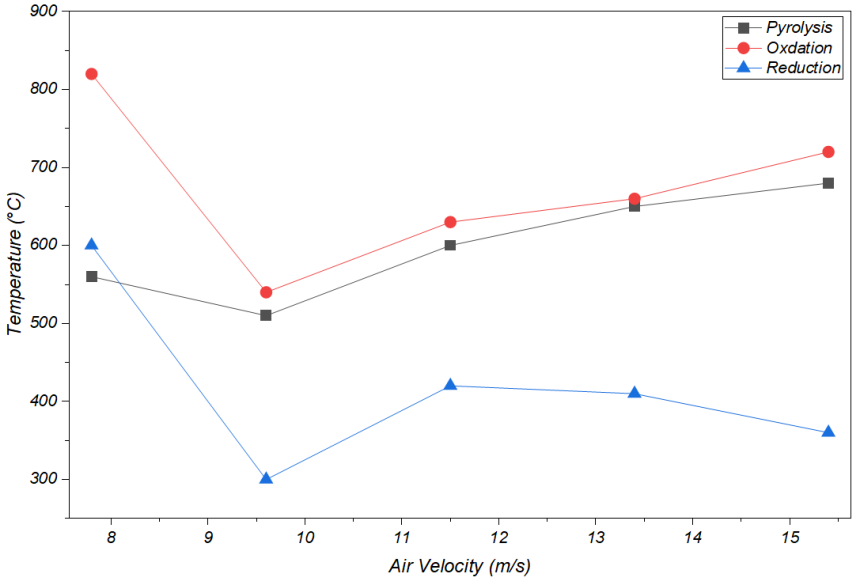

Figure 4. Temperature graph in each zone (pyrolysis, oxidation, reduction).

reduction zone down to ±300 °C, indicating that the cooling effect of airflow was more dominant than the heat generated from oxidation reactions. At medium airflow rates (11.5–13.4 m/s), the temperatures in the pyrolysis zone (550–600 °C) and reduction zone (460–480 °C) rose again, while the oxidation zone stabilized within the range of 630 – 660 °C, suggesting a balance between sufficient oxygen supply to support combustion reactions and the cooling effect of the airflow. At the highest airflow rate of 15.4 m/s, the oxidation peak increased again to ±710 °C, with the pyrolysis and reduction zones also relatively stable (620 °C and 520 °C, respectively), indicating that under this condition, the abundant oxygen supply enhanced the intensity of exothermic reactions despite the presence of cooling effects. Scientifically, these results confirm that AFR is a critical parameter influencing the temperature profile in each gasification zone: too low an airflow results in higher heat accumulation but limited oxygen supply, while too high an airflow reduces thermal efficiency due to excessive cooling. Therefore, an optimum airflow rate is required to maintain a balance between heat generation in the oxidation zone and sufficient temperature availability in the pyrolysis and reduction zones, in order to produce syngas of the best quality.

B. Heating time response

Figure 5 illustrates the relationship between heating time and temperature rise in the gasification system under varying air flow rates of 7.8 m/s, 9.6 m/s, 11.5 m/s, 13.4 m/s, and 15.4 m/s. In the initial phase (0–5

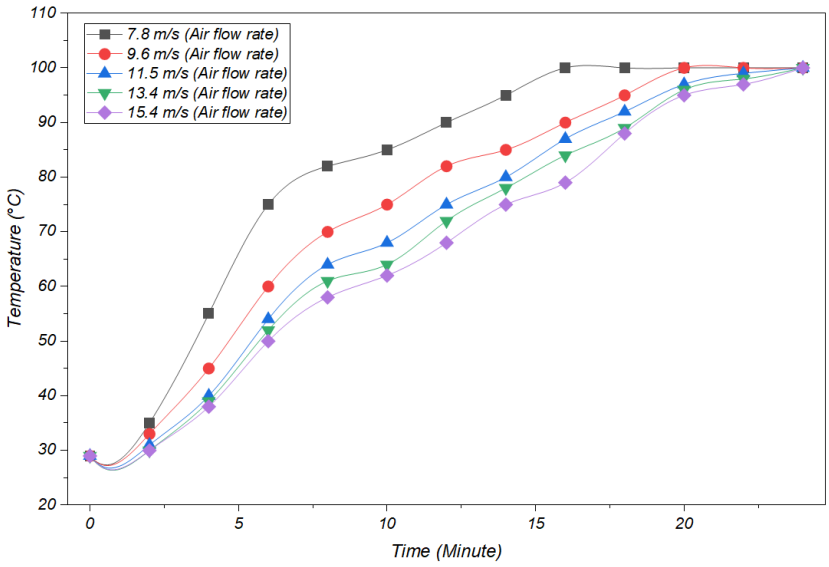

Figure 5. Comparison of water boiling temperature using corncob as feedstock.

minutes), the airflow rate of 7.8 m/s produced the fastest temperature increase, reaching approximately 75 °C at the fifth minute, while higher airflow rates showed slower increases due to the cooling effect of the incoming air. In the intermediate phase (5–15 minutes), the temperature continued to rise at a more stable rate, with higher airflow rates resulting in slower temperature increases. In the final phase (15–22 minutes), all temperature curves tended to converge toward approximately 100 °C, indicating that the system had reached a steady state. This finding suggests that airflow rate has a significant effect during the initial heating phase of the reactor; however, under steady state conditions, its influence becomes less pronounced as the system achieves thermal equilibrium.

C. PV power profile

Figure 6 illustrates the relationship between time and the output power of the solar panel from 07:00 to 16:00, displaying an inverted parabolic pattern that reflects the typical daily variation of solar irradiance. The measurements were conducted in Gorontalo Province, Indonesia (0.54° N, 123.06° E) in August 2025, which climatologically corresponds to the peak of the dry season when solar radiation levels are relatively high and stable. At around 07:00, the output power remains low, approximately 60 W, due to the low solar elevation angle.

The power then increases sharply, exceeding 450 W between 09:00 and 10:00, and reaches its peak of about ±730-750W at approximately 12:00–12:30, when the sun is nearly perpendicular to the panel surface and the output approaches the panel's rated peak capacity of 600 WP. After midday, the output gradually decreases as the solar incidence angle declines, accompanied by increased atmospheric scattering and the possible presence of thin afternoon clouds. By 16:00, the output drops significantly to around <100 W.

This diurnal pattern confirms that the solar panel system operates at its optimal performance around solar noon. The asymmetry between the morning rise and afternoon decline also indicates the influence of panel thermal effects, local atmospheric dynamics, and surrounding environmental or operational conditions. Furthermore, the area under the curve can be used to estimate the total daily electrical energy generated and to evaluate the system's feasibility in meeting the required load demand.

Climatologically, annual variability in solar irradiance in Gorontalo is relatively small compared to higher latitude regions because it is located in the tropical zone near the equator. However, maximum irradiance typically occurs between June and October during the dry season, whereas slight reductions take place between December and February due to increased cloud cover. Therefore, the August 2025 dataset used in this graph represents a period of high and stable solar radiation, making it ideal for evaluating the performance of the solar panel system.

D. Energy and exergy efficiency

Figure 7 shows the relationship between preheating temperature and energy and exergy efficiency across the range of 650–1000 °C. In general, both efficiency parameters exhibit a consistent upward trend as the preheating temperature increases, indicating that the thermal process becomes more advantageous at higher operating temperatures.

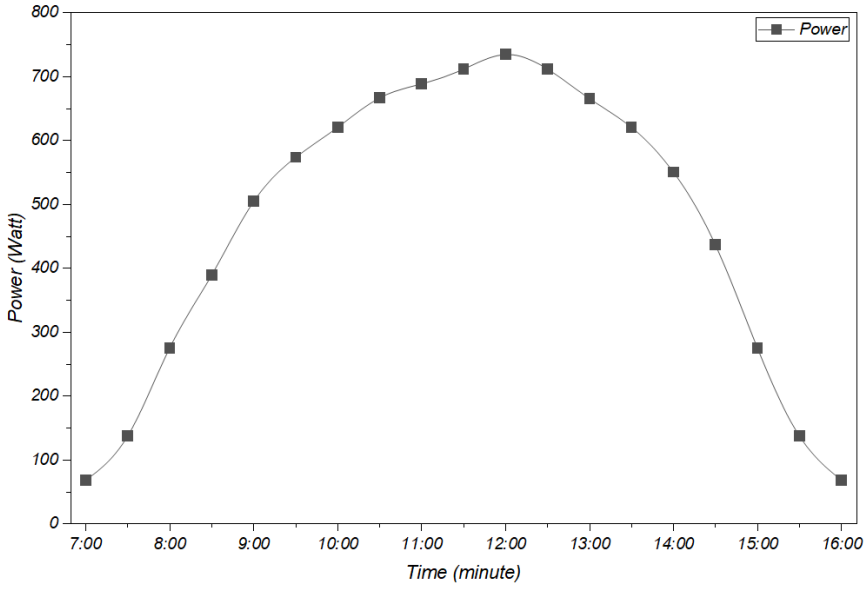

Figure 6. Comparison of PV panel output power with solar irradiance.

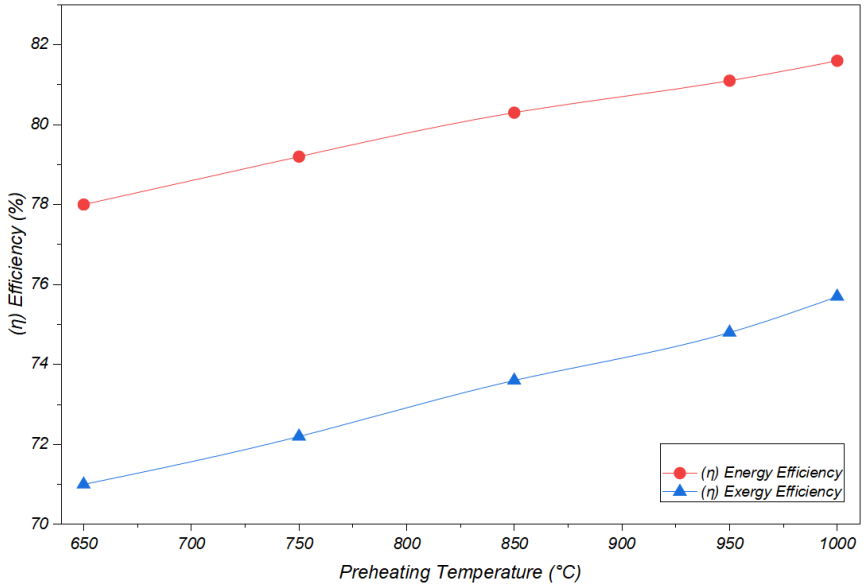

Figure 7. Effect of initial heating temperature on energy and exergy efficiency in thermal systems.

Based on the graph illustrating the relationship between preheating temperature and both energy and exergy efficiency, it is evident that both parameters increase consistently within the range of 650–1000 °C. The energy efficiency rises from approximately 71 % to 75.7 % as the temperature increases, indicating that higher preheating temperatures enhance the utilization of energy within the system. Thermodynamically, higher preheating temperatures improve heat transfer rates and increase the effectiveness of thermal reactions, allowing a greater portion of energy to be converted into useful work. Meanwhile, the exergy efficiency exhibits higher values compared to energy efficiency, increasing from around 78 % to 82 % over the same temperature range. This trend reflects an improvement in the quality of energy available for performing work as the temperature increases, owing to the larger temperature difference between the system and its surroundings, which enhances the system's work potential. The uniform upward trend in both parameters also indicates reduced process irreversibilities at higher temperatures, including diminished heat losses and entropy generation. The difference between energy and exergy efficiency, which remains within the range of 6–7 %, is typical and illustrates that although the total available energy can be utilized, not all of it possesses the same quality for producing work. Overall, the graph demonstrates that increasing the preheating temperature has a positive and significant impact on the thermal performance of the system. Therefore, operating at higher temperatures, such as 900–1000 °C, may be considered an optimal range, provided that material limitations and operational constraints are taken into account.

E. Limitations and implications

The limitations of this study are primarily associated with the laboratory scale updraft reactor used, which means that the temperature profile, airflow distribution, and syngas quality obtained may differ when applied to pilot-scale or industrial systems that involve larger dimensions and more complex thermal behavior. In addition, the power supply provided by the 600 WP PV system is highly dependent on weather conditions and fluctuations in solar irradiance, causing its performance in real outdoor environments to vary more significantly than in the controlled experimental setting. Instrumentation limitations may also introduce measurement deviations. These constraints can influence the applicability of the results in real-world scenarios, particularly in estimating thermal efficiency, flame stability, and long-term operational sustainability. Therefore, field implementation should consider the use of larger reactor designs, more precise AFR control systems, higher capacity PV units with adequate energy storage, and long-duration testing to ensure practical reliability of the integrated system.

IV. Conclusion

This study demonstrates that integrating corncob-fueled updraft gasification with a photovoltaic (PV) solar power system offers a technically feasible, efficient, and sustainable hybrid energy solution for small-scale applications, especially in rural areas with abundant biomass resources. The experimental results confirm that air flow rate (AFR) plays a critical role in determining the temperature distribution across the drying, pyrolysis, oxidation, and reduction zones, with

optimal performance achieved at AFR values of 11.5–13.4 m/s, resulting in stable temperature profiles and improved syngas quality. The 600 WP PV system successfully supplied the electrical power required for the blower, pump, and instrumentation, highlighting its potential for autonomous off-grid operation. These findings support practical applications in household energy, micro-scale industries, and decentralized renewable energy systems, while also emphasizing the value of utilizing agricultural residues such as corncobs. However, further research is needed to address limitations such as tar reduction techniques, multi-stage air supply configurations, enhanced PV battery integration, and predictive modeling for system optimization, enabling this hybrid PV gasifier system to serve as a more reliable and scalable renewable energy alternative.

Declarations

Author contribution

Rifaldo Pido contributed to the conceptualization of research, investigation, formal analysis, visualization, drafting of the original manuscript, manuscript review and editing, as well as overall supervision of the research implementation. **Steven Humena** was involved in conceptualization, investigation, data validation, data curation, and contributed to drafting the original manuscript as well as manuscript review and editing. **Fadhil Abdullah** was responsible for advanced formal analysis, provision of resources, software development and utilization, and acquisition of research funding.

Funding statement

The authors would like to express their gratitude for the research grant support from the Ministry of Research, Technology, and Higher Education of Indonesia through the 2025 Regular Fundamental Research (PFR) scheme with contract number 857/LL16/AL.04/2025.

Competing interest

The authors declare that they have no known competing financial interests or personal relationships that could have appeared to influence the work reported in this paper.

The use of AI or AI-assisted technologies

The authors declare that no AI or AI-assisted technologies were used.

Additional information

References

[1] K. Siregar *et al.*, "Life cycle impact assessment on electricity production from biomass power plant system through life cycle assessment (LCA) method using biomass from palm oil mill in Indonesia," *E3S Web Conf.*, vol. 188, p. 18, 2020.

[2] A. S. Adewuyi and K. H. Lasisi, "Design and fabrication of a laboratory scale updraft gasifier," *J. Appl. Sci. Environ. Manag.*, vol. 23, no. 11, p. 1915, 2020.

[3] F. Z. Mansur, C. K. M. Faizal, A. Samad, S. M. Atnaw, and S. A. Sulaıman, "Performance modelling and validation on co-gasification of coal and sawdust pellet in research-scale downdraft reactor," in *IOP Conference Series Materials Science and Engineering*, IOP Publishing, 2019, p. 12023.

[4] S. Lotfi, "Technologies for Tar removal from biomass-derived syngas," *Pet. Petrochemical Eng. J.*, vol. 5, no. 3, pp. 1–35, 2021.

[5] S. Thapa, P. Bhoi, A. Kumar, and R. L. Huhnke, "Effects of syngas cooling and biomass filter medium on tar removal," *Energies*, vol. 10, no. 3, p. 349, 2017.

[6] A. Vulpio, N. Casari, M. Morini, M. Pinelli, and A. Suman, "Numerical investigation of a wood-chip downdraft gasifier," *E3S Web Conf.*, vol. 113, p. 1002, 2019.

[7] S. Piazzi, X. Zhang, F. Patuzzi, and M. Baratieri, "Techno-economic assessment of turning gasification-based waste char into energy: A case study in South-Tyrol," *Waste Manag.*, vol. 105, pp. 550–559, 2020.

[8] H. Yang *et al.*, "Evaluation of engineered biochar-based catalysts for syngas production in a biomass pyrolysis and catalytic reforming process," *Energy & Fuels*, vol. 37, no. 8, pp. 5942–5952, 2023.

[9] M. A. Partogi, I. G. B. W. Kusuma, and K. Astawa, "Analisa unjuk kerja sistem PLTG di PT Indonesia Power Unit Pembangkitan Bali," *J. METTEK*, vol. 4, no. 1, p. 16, 2018.

[10] K. Laouidi, S. Habchi, C. K. Fanezouné, B. Sallek, K. Nataliia, and H. El Bari, "Advancements in artificial neural networks and fast pyrolysis of biomass processing: A comprehensive review and a bibliometric analysis," *Journal of Analytical and Applied Pyrolysis*. Elsevier BV, p. 107098, 2025.

[11] J. Ji *et al.*, "Optimization and uncertainty analysis of co-combustion ratios in a semi-isolated green energy combined cooling, heating, and power system (SIGE-CCHP)," *Energy*, vol. 302, p. 131784, 2024.

[12] L. V Martinez, J. E. Rubiano, M. Figueredo, and M. F. Gómez, "Experimental study on the performance of

gasification of corncobs in a downdraft fixed bed gasifier at various conditions," *Renew. Energy*, vol. 148, pp. 1216–1226, 2020.

[13] J. A. Martillo Aseffe, A. Martinez González, R. Lesme Jaén, and E. E. Silva Lora, "The corn cob gasification-based renewable energy recovery in the life cycle environmental performance of seed-corn supply chain: An Ecuadorian case study," *Renew. Energy*, vol. 163, pp. 1523–1535, 2021.

[14] D. Xu, X. Gu, and Y. Dai, "Concentrating solar assisted biomass-to-fuel conversion through gasification : A review," *Front. Energy Res.*, no. January, pp. 1–26, 2023.

[15] Y. Xin, X. Xing, X. Li, and H. Hong, "Integrating solar-driven biomass gasification and PV–electrolysis for sustainable fuel production: Thermodynamic performance, economic assessment, and CO2 emission analysis," *Chem. Eng. J.*, vol. 497, p. 153941, 2024.

[16] E. Jadidi, M. H. Khoshgoftar Manesh, M. Delpisheh, and V. C. Onishi, "Advanced exergy, exergoeconomic, and exergoenvironmental analyses of integrated solar-assisted gasification cycle for producing power and steam from heavy refinery fuels," *Energies*, vol. 14, no. 24, 2021, doi: 10.3390/en14248409.

[17] Y. Zhuang and A. Wang, "The mechanical properties and micro-mechanism of xanthan gum–coconut shell fiber composite amended soil," *Buildings*, vol. 15, no. 11, p. 1781, 2025.

[18] İ. V. Sezgin and H. Merdun, "Estimation of fast pyrolysis product yields of different biomasses by artificial neural networks," *Process Saf. Environ. Prot.*, 2025.

[19] R. Ochieng and S. Sarker, "Energy and techno-economic analysis of integrated supercritical water gasification of sewage sludge and fast pyrolysis of wood for power, heat, and hydrogen production," *Chem. Eng. Sci.*, p. 121236, 2025.

[20] H. Elshareef *et al.*, "Bio-energy potential of cotton stalks via thermal technologies: a review," *Journal of Cotton Research*, vol. 8, no. 1. BioMed Central, 2025.

[21] M. Triani *et al.*, "Mapping analysis of biomass potential on Java Island for supporting power plant: A review," *E3S Web of Conferences*, vol. 519. EDP Sciences, p. 2012, 2024.

[22] S. A. Razzak, M. Khan, F. Irfan, M. A. Shah, A. Nawaz, and M. M. Hossain, "Catalytic co-pyrolysis and kinetic study of microalgae biomass with solid waste feedstock for sustainable biofuel production," *J. Anal. Appl. Pyrolysis*, p. 106755, 2024.

[23] R. P. Devi, S. Kamaraj, R. Angeeswaran, and S. Pugalendhi, "Tar and particulate removal methods for the producer gas obtained from biomass gasification," *Int. J. Curr. Microbiol. Appl. Sci.*, vol. 6, no. 10, pp. 269–284, 2017.

[24] K. X. Kallis, G. A. P. Susini, and J. E. Oakey, "A comparison between Miscanthus and bioethanol waste pellets and their performance in a downdraft gasifier," *Appl. Energy*, vol. 101, pp. 333–340, 2012.

[25] B. Ghosh and S. Mandal, "Enhanced solar PV cell parameter identification via particle swarm optimization (PSO) with weighted objective function," *J. Mechatronics, Electr. Power, Veh. Technol.*, vol. 16, no. 1, pp. 15–26, 2025.